Articles

Stable and Efficient Fluorescent Red and Green Dyes for External and Internal Conversion of Blue OLED Emission

Sally A. Swanson,* Greg M. Wallraff, Jian P. Chen, Weijie Zhang, Luisa D. Bozano, Kenneth R. Carter, Jesse R. Salem, Reymundo Villa, and J. Campbell Scott

IBM Research Divison, Almaden Research Center, San Jose, California 95120-6099

Received October 28, 2002. Revised Manuscript Received February 25, 2003

We have synthesized a series of diphenylamine-substituted coumarin, (dicyanomethylene)-pyran, and benzophenoxazone dyes and report on their optical and electroluminescent properties, thermal and photooxidative stabilities, and potential as red and green dopants for organic light-emitting diode (OLED) displays or down-conversion fluorescent dyes for external color-converters. Incorporation of the bulky phenyl groups in these dyes delays the onset of concentration quenching when they are dissolved in polymer films. Their improved photoluminescent efficiency and photooxidative stability make them excellent candidates for external color-conversion. The improved electroluminescence and power efficiencies and enhanced thermal stability of 3-(2′-benzimidazolyl)-7-(diphenylamino)-2*H*-1-benzopyran-2-one (C7S) as well as its Commission Internationale d'Eclairage (CIE) coordinates suggests its use as a green dopant in OLED devices.

Introduction

Organic light-emitting diodes (OLEDs) are beginning to enter the marketplace, and with their relatively simple structure and low-power requirements may have the potential to replace liquid crystal technology in portable flat-panel display applications.[1,2] However, despite much recent progress, the inexpensive fabrication of full-color high-resolution OLED displays remains a challenge. Many approaches to full-color OLED displays have been proposed: utilizing an emitter whose color of electroluminescence (EL) is voltage dependent;[3−8] using separate red, green, and blue emitters[9−11] or stacking separate red, green, and blue emitter structures;[12,13] using a white emitter with individually patterned color filters[14−16] or with microcavity structures;[17−20] and using a blue emitter with individually patterned fluorescent materials to "down-convert" to the red and green colors.[21−25] In this last strategy, the down-conversion may be realized either externally with a separate color-conversion layer[21−23] or within the OLED device structure by dye doping the small molecule[24] or polymer[25]emitter layer itself. The use of a single blue-emitter layer and down-converting the emission color with fluorescent dyes offers the combination of full-color gamut, high-resolution, good viewing angle, and relatively flexible and simple processing while maintaining

* To whom correspondence should be addressed. Phone: 408-927-1629. Fax: 408-927-3310. E-mail: saswans@almaden.ibm.com.

(1) Allen, K. *Solid State Technol.* **2001**, *44* (8), 42.
(2) Anon. *Solid State Technol.* **2001**, *44* (10), 22.
(3) Berggren, M.; Inganäs, O.; Gustafsson, G.; Rasmusson, J.; Andersson, M. R.; Hjertberg, T.; Wennerström, O. *Nature* **1994**, *372*, 444.
(4) Granström, M.; Inganäs, O. *Appl. Phys. Lett.* **1996**, *68*, 147.
(5) Tasch, S.; Niko, A.; Leising, G.; Scherf, U. *Appl. Phys. Lett.* **1996**, *68*, 1090.
(6) Yoshida, M.; Fujii, A.; Ohmori, Y.; Yoshino, K. *Jpn. J. Appl. Phys.* **1996**, *35*, L397.
(7) Hamaguchi, M.; Yoshino, K. *Appl. Phys. Lett.* **1996**, *69*, 143.
(8) Yoshida, M.; Fujii, A.; Ohmori, Y.; Yoshino, K. *Appl. Phys. Lett.* **1996**, *69*, 734.
(9) Tang C. W.; Van Slycke, S. A. *Appl. Phys. Lett.* **1987**, *51*, 913.
(10) Tokailin, H.; Hosokawa, C.; Kusomoto, T. U.S. Patent 5,126,-214, 1992.
(11) Wu, C. C.; Sturm, J. C.; Register, R. A.; Thompson, M. E. *Appl. Phys. Lett.* **1996**, *69*, 3117.
(12) Shen, Z.; Burrows, P. E.; Bulovic, V.; Forrest, S. R.; Thompson, M. E. *Science* **1997**, *276*, 2009−2011.
(13) Forrest, S. R.; Thompson, M. E.; Burrows, P. E.; Sapochak, L. S.; McCarty, D. M. U.S. Patent 5,757,026, 1998.
(14) Kido, J.; Hongawa, K.; Okuyama K.; Nagai, K. *Appl. Phys. Lett.* **1994**, *64*, 615.
(15) Kido, J.; Kimura, M.; Nagai, K. *Science* **1995**, *267*, 1332.
(16) Kido, J.; Ikeda, W.; Kimura, M.; Nagai, K. *Jpn. J. Appl. Phys.* **1996**, *35*, L394.
(17) Dodabalapur, A.; Rothberg, L. J.; Miller, T. M.; Kwock, E. W. *Appl. Phys. Lett.* **1994**, *64*, 2486.
(18) Dodabalapur, A.; Rothberg, L. J.; Miller, T. M. *Electron. Lett.* **1994**, *30*, 1000.
(19) Dodabalapur, A.; Rothberg, L. J.; Miller, T. M. *Appl. Phys. Lett.* **1994**, *65*, 2308.
(20) Nakayama, T. *Opt. Rev.* **1995**, *2*, 39.
(21) Tokailin, H.; Hosokawa, C.; Kusomoto, T. U.S. Patent 5,126,-214, 1992.
(22) Tang, C. W.; Williams, D. J.; Chang, J. C. U.S. Patent 5,294,-870, 1994.
(23) Tasch, S.; Brandstätter, C.; Meghdadi, F.; Leising, G.; Froyer, G.; Athouel, L. *Adv. Mater.* **1997**, *9*, 33.
(24) Tang, C. W.; Van Slyke, S. A.; Chen, C. H. *J. Appl. Phys.* **1989**, *65*, 3610.
(25) Johnson, G. E.; McGrane, K. M.; Stolka, M. *Pure Appl. Chem.* **1995**, *67*, 761.

10.1021/cm021056q CCC: $25.00
Published on Web 05/17/2003

Chart 1. Molecular Structures of Commercial Dyes

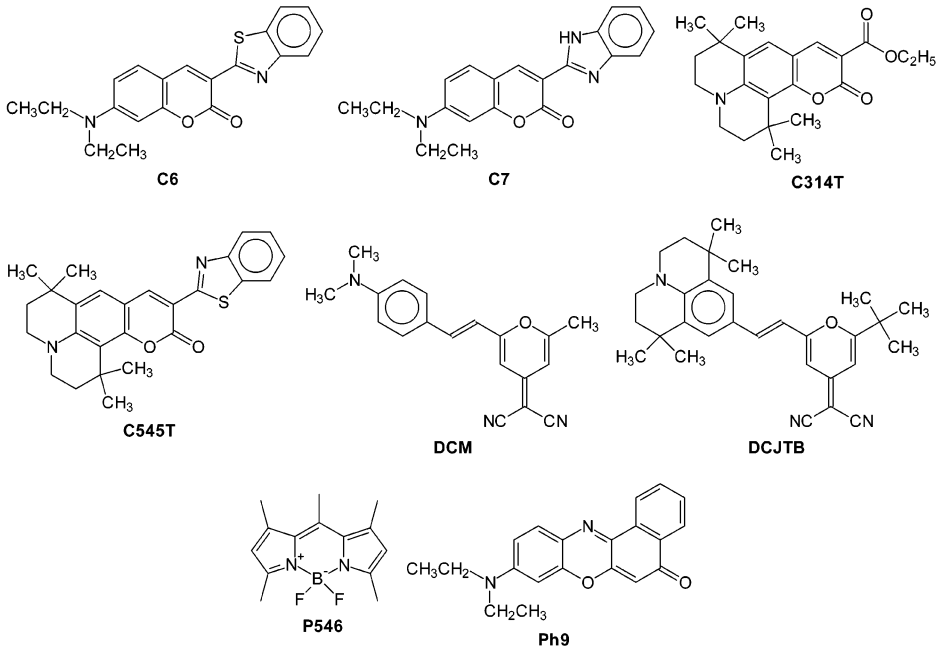

efficiency. The two down-conversion schemes, external color conversion and internal dye doping, are depicted in Figure 1.

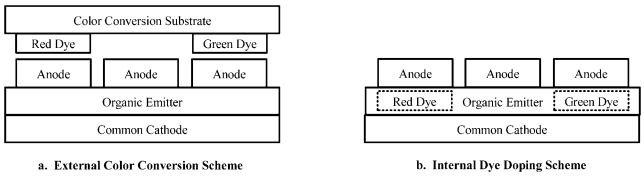

Figure 1. Down-conversion color schemes. External color-conversion (a) is depicted emitting up through a transparent anode into a separate converter structure. Internal dye doping (b) emission can be either up or down through either electrode.

In full-color emissive displays, sub-pixels emit red, green, and blue light. Utilizing a single blue-emitting layer, the blue sub-pixels require no color-conversion or doping. In the red and green sub-pixels, the blue excitation should be either absorbed by the color-converter layers in external conversion or transferred to the dopant dyes in internal conversion resulting in emitted light at the desired wavelength (red or green).

In both external and internal conversion instances, the luminescent efficiency and photooxidative stability of the dyes is essential to the success of color-conversion. Prior work on enhancing the luminance and stability of dopant dyes involved rigidizing the alkylamino donor moieties via cyclization to the julolidine ring, adding steric spacers to minimize dye−dye interaction at high dopant concentrations, and (in the case of (dicyanomethylene)pyran (DCM)-type dyes) eliminating bis-condensation products.[26−28] In this paper we present a series of coumarin, (dicyanomethylene)pyran, and benzophenoxazone dyes designed specifically for color-conversion. These dyes differ from their commercial counterparts by the incorporation of diarylamine groups, leading to enhanced efficiency and stability over their dialkylamino analogues (Chart 1). We refer to them by adding the suffix, S, to the name of their commercial counterparts. Although some S-class and related dyes have been previously described,[29−35] this is the first detailed study of their spectral properties and thermal stability. Because the emissive dyes must be patterned, we also examine the properties of OLED devices in which the dopant is transferred to the polymer layer during contact with a dye-doped elastomeric stamp.

Experimental Section

Materials. 3-(2′-Benzothiazolyl)-7-(diethylamino)-2*H*-1-benzopyran-2-one (C6), 9-diethylamino-5*H*-benzo[*a*]phenoxazin-5-one (Ph9), and 4,4-difluoro-1,3,5,7,8-pentamethyl-4-bora-3a,4a-diaza-s-indacene (P546) were purchased from Lambda Physik. 3-(2′-Benzimidazolyl)-7-(diethylamino)-2*H*-1-benzopyran-2-one (C7), 4-(dicyanomethylene)-2-methyl-6-(*p*-dimethylaminostyryl)-4*H*-pyran (DCM), 10-(2-benzothiazolyl)-2,3,6,7-tetrahydro-1,1,7,7-tetramethyl-1*H*,5*H*,11*H*-(1)benzopyrano-(6,7, 8-*ij*)quinolizin-11-one (C545T), 2,3,6,7-tetrahydro-1,1,7,7-tetramethyl-11-oxo-1*H*,5*H*,11*H*-(1)benzopyrano(6,7, 8-*ij*)quinolizine-10-carboxylic acid ethyl ester (C314T), and 2-(1,1-dimethylethyl)-6-(2-(2,3,6,7-tetrahydro-1,1,7,7-tetramethyl-1*H*,5*H*-benzo(*ij*)quinolizin-9-yl)ethenyl)-4*H*-pyran-4-ylidene)-propanedinitrile (DCJTB) were purchased from Kodak. *p*-Diphenylaminobenzaldehyde was obtained from Hodogaya Chemical Co., Ltd. 4-Dicyanomethylene-2,6-dimethyl-4-*H*-pyran was synthesized as reported in the literature.[36,37]

(26) Chen, C. H.; Tang, C. W.; Shi, J.; Klubek, K. P. *Thin Solid Films* **2000**, *363*, 327.
(27) Tao, X. T.; Miyata, S.; Sasabe, H.; Zhang, G. J.; Wada, T.; Jiang, M. H. *Appl. Phys. Lett.* **2001**, *78*, 279.
(28) Chen, C. H.; Tang, C. W. *Appl. Phys. Lett.* **2001**, *79*, 3711.
(29) Karasawa, A.; Ito, N.; Oguchi, T. Jpn. Kokai Tokkyo Koho 04-225364, 1992.
(30) Mitekura, H.; Danoh, Y.; Ooga, Y.; Mori, N.; Suga, S.; Taniguchi, Y.; Koyama, T.; Adachi, C.; Saitou, T.; Satsuki, M. Patent. WO 99/40086, 1999; EP 1,052,261, 2000.
(31) Tamano, M. Jpn. Kokai Tokkyo Koho 2000-328052, 2000.
(32) Zheng, S.; Shi, J.; Klubek, K. P. U.S. Patent 6,268,072, 2001.
(33) Kobori, I.; Ohisa, K.; Nakaya, K. Inoue, T. U.S. Patent 6,285,-039, 2001.
(34) Hironaka, Y.; Terada, I.; Tagami, S. Jpn. Kokai Tokkyo Koho 2001-102174, 2001.
(35) Swanson, S. A.; Wallraff, G. M. U.S. Patent Application 2002/0127428, 2002.
(36) Woods, L. L. *J. Am. Chem. Soc.* **1958**, *80*, 1440.
(37) Ohta, M.; Kato, H. *Bull. Chem. Soc. Jpn.* **1959**, *32*, 707.

^{1}H NMR spectra were obtained on a Bruker AC250 or Avance 400 spectrometer and referenced to the deuterated solvent.

3-Methoxytriphenylamine (3). 37.34 g (0.3 mol) of *m*-anisidine **(1)**, 142.47 g (0.7 mol) of iodobenzene **(2)**, 74.93 g (1.2 mol) of copper powder, 2.20 g (8 mmol) of 18-crown-6, and 320.8 g (2.3 mol) of anhydrous potassium carbonate in 500 mL of phenyl ether were placed into a 1-L three necked round-bottom flask equipped with overhead stirrer, reflux condenser, nitrogen inlet, thermowell, and heating mantle, and heated at reflux overnight. The solids were removed by filtration, and the solvents were removed by vacuum distillation. The resulting 82 g (98% crude yield) of brown oil was used in the next step. ^{1}H NMR ($CDCl_3$, 250 MHz): δ [ppm] 3.70 (s, 3H, CH_3); 6.55 (dd, $J_{4,5} = 7.2$ Hz and $J_{4,6} = 2.1$ Hz, 1H, H^4); 6.60−6.67 (m, 2H, H^2 + H^6); 6.87−7.30 (m, 11H, H^5 + ArH).

3-Hydroxytriphenylamine (4). Aluminum (9.92 g (0.37 mol)), 140 g (0.55 mole) of iodine, and 200 mL of acetonitrile were placed in a three-necked 500-mL round-bottom flask equipped with magnetic stirring, a reflux condenser, nitrogen inlet, and an addition funnel containing 82 g (0.3 mol) of **3** dissolved in 100 mL of acetonitrile. The mixture was refluxed with stirring until the purple color of the iodine disappeared. The solution of **3** was then added and the resulting mixture was refluxed overnight. After cooling, the reaction mixture was poured onto ice and extracted into ether. The ether phase was washed with sodium hydrosulfite, dried over magnesium sulfate, filtered, rotary evaporated to remove solvent, and dried in a vacuum oven to 73.6 g (100% crude yield) of oil which was used in the next step. ^{1}H NMR ($CDCl_3$, 250 MHz): δ [ppm] 5.13 (b, 1H, OH); 6.44 (dd, $J_{4,5} = 7.9$ Hz and $J_{4,6} = 2.1$ Hz, 1H, H^4); 6.51 (t, $J_{2,6} = 2.1$ Hz, 1H, H^2); 6.61 (dd, $J_{2,6} = 2.1$ Hz and $J_{5,6} = 8.0$ Hz, 1H, H^6); 6.87−7.30 (m, 11H, H^5 + ArH).

3-Carboethoxy-7-(diphenylamino)-2*H*-1-benzopyran-2-one (C314S). Compound **4** (73.86 g (0.3 mol)) and 69.95 g (0.32 mol) of diethyl ethoxymethylenemalonate (**5**) were dissolved in 200 mL of THF in a 1-L three-necked round-bottom flask equipped with reflux condenser, heating mantle, magnetic stirrer, and a flexible tube connected to a 100-mL round-bottom flask containing 43 mL (0.39 mole) of titanium(IV) chloride which was added quickly but slow enough to prevent overheating. The mixture was allowed to reflux overnight. The cooled mixture was poured into 3 L of water containing 18 mL of concentrated hydrochloric acid and followed by extraction into methylene chloride. The organics were washed with water, 1 N sodium hydroxide, and water, dried over magnesium sulfate, filtered, rotary evaporated to remove solvent, yielding 120 g C314S as an oil. The product was further purified by flash chromatography on silica gel using methylene chloride as the eluent to 52 g (46% yield) of orange glass. ^{1}H NMR ($CDCl_3$, 250 MHz) δ [ppm]: 1.37 (t, $J = 7.1$ Hz, 3H, CH_3); 4.36 (q, $J = 7.1$ Hz, 2H, CH_2); 6.70 (d, $J_{6,8} = 2.0$ Hz, 1H, H^8); 6.83 (dd, $J_{5,6} = 8.6$ Hz and $J_{6,8} = 2.0$ Hz, 1H, H^6); 7.13−7.40 (m, 11H, H^5 + ArH); 8.42 (s, 1H, H^4). Anal. Calcd for $C_{24}H_{19}NO_4$: C, 74.8; H, 5.0; N, 3.6. Found: C, 74.8; H, 5.28; N, 3.29.

7-(Diphenylamino)-2*H*-1-benzopyran-2-one 3-carboxylic Acid (C343S). C314S (30 g (78 mmol)) was dissolved in 200 mL of methanol in a 500-mL round-bottom flask equipped with a reflux condensor, magnetic stirrer, and heating mantle. The solution was taken to reflux, 187 mL of 0.5 N NaOH solution was added, and the mixture was taken to reflux again and then allowed to cool to room temperature. HCl (2 N) was added to acidify the solution, and the organics were extracted into ether, washed with 2 N HCl and water, transferred to a 500-mL round-bottom flask and rotary evaporated to remove solvent. A 500-mL portion of methanol was added and the solid was triturated overnight. The solid product was filtered and dried under vacuum to give 7.2 g of yellow solid (26% crude product yield) which was further purified by recrystallization from CH_2Cl_2/methanol. ^{1}H NMR ($CDCl_3$, 250 MHz) δ [ppm]: 6.75 (dd, $J_{6,8} = 2.5$ Hz and $J_{4,8}$=0.6 Hz, 1H, H^8); 6.89 (dd, $J_{5,6} = 8.9$ Hz and $J_{6,8} = 2.3$ Hz, 1H, H^6); 7.18−7.44 (m, 11H, H^5 + ArH); 8.70 (d, $J_{4,8}$=0.5 Hz, 1H, H^4); 12.25 (s, br, 1H, COOH). Anal. Calcd for $C_{22}H_{15}NO_4$: C, 73.9; H, 4.2; N, 3.9. Found: C, 73.47; H, 4.3; N, 3.86.

3-(2′-Benzothiazolyl)-7-(diphenylamino)-2*H*-1-benzopyran-2-one (C6S). C314S (7.5 g (19.5 mmol)), 2.45 g (19.6 mmol) of 2-aminothiophenol **(6)**, 15 g of diphenyl, and 15 g of phenyl ether were placed in a 50-mL round-bottom flask and taken to reflux for 30 min. After the mixture cooled to room temperature, 50 mL of toluene was added, and the product was isolated by filtration, washed with ether, dried in a vacuum to 2.7 g (31% crude product yield), and recrystallized from methylene chloride/ethyl acetate to yield 2.0 g of orange crystals (23% overall yield). ^{1}H NMR ($CDCl_3$, 250 MHz) δ [ppm]: 6.84 (d, $J_{6,8} = 2.2$ Hz, 1H, H^8); 6.90 (dd, $J_{5,6} = 8.9$ Hz and $J_{6,8} = 2.2$ Hz, 1H, H^6); 7.17−7.61 (m, 11H, H^5 + ArH); 7.94 (d, $J_{4',5'} = 7.9$ Hz 1H, H$^{4'}$); 8.04 (d, $J_{6',7'} = 8.1$ Hz, 1H, H$^{7'}$); 8.96 (s, 1H, H^4). Anal. Calcd for $C_{28}H_{18}N_2O_2S$: C, 75.3; H, 4.1; N, 6.3; S, 7.2. Found: C, 75.27; H, 4.57; N, 5.29; S, 6.16.

3-(2′-Benzimidazolyl)-7-(diphenylamino)-2*H*-1-benzopyran-2-one (C7S). A solution of 7.9 mL (47 mmol) of triflic anhydride in 150 mL of methylene chloride was added to a solution of 26.16 g (94 mmol) of triphenylphosphine oxide in 150 mL of methylene chloride at 0 °C under nitrogen atmosphere. The resulting mixture was allowed to come to room temperature, and a solution of 2.54 g of *o*-phenylenediamine **(7)** and 7 g (19.6 mmol) of C343S in 80 mL of methylene chloride was added dropwise. The slurry was stirred overnight. The reaction mixture was washed with 5% sodium bicarbonate, water, and brine, dried over magnesium sulfate, filtered, and rotary evaporated to remove the solvent. The product was purified by flash column chromatography in methylene chloride to yield 4 g (48% crude product yield). Further purification by recrystallization yielded 2.21 g of orange crystals (26% overall yield). ^{1}H NMR ($CDCl_3$, 400 MHz) δ [ppm]: 6.84 (d, $J_{6,8} = 2.1$ Hz, 1H, H^8); 6.96 (dd, $J_{5,6} = 8.6$ Hz and $J_{6,8} = 2.1$ Hz, 1H, H^6); 7.22−7.29 (m, 6H, ArH); 7.32 (q, $J_{4',5'} = 3$ Hz 2H, H$^{4'}$ + H$^{5'}$); 7.38−7.44 (m, 4H, ArH); 7.48 (d, $J_{5,6} = 8.6$ Hz, H^5); 7.55 (b, 1H, H$^{4'}$); 7.80 (b, 1H, H$^{7'}$); 9.06 (s, 1H, H^4); 11.32 (b, 1H, NH). Anal. Calcd for $C_{28}H_{19}N_3O_2$: C, 78.3; H, 4.5; N, 9.8. Found: C, 70.06; H, 4.23; N, 8.56.

4-(Dicyanomethylene)-2-methyl-6-(*p*-diphenylaminostyryl)-4*H*-pyran (DCMS). 4-Dicyanomethylene-2,6-dimethyl-4-*H*-pyran (**8**) (17.22 g (0.1 mol)), 27.33 g (0.1 mol) of *p*-diphenylaminobenzaldehyde **(9)**, 8.51 g (0.1 mol) of piperidine, and 250 mL of 1-propanol were combined and refluxed under nitrogen overnight. After the solution cooled, the dimer, 4-(dicyanomethylene)-2,6-bis(*p*-(diphenylamino)-styryl)-4*H*-pyran (DADP), precipitated and was removed by filtration. The filtrate was rotary evaporated to remove solvent and the product was recrystallized from methylene chloride/ethyl acetate/hexane to 2.1 g of red−brown crystals (5% yield). ^{1}H NMR ($CDCl_3$, 400 MHz) δ [ppm]: 2.42 (s, 3H, CH_3); 6.54 (s, 1H); 6.65 (d, $J = 2.0$ Hz); 7.04 (d, $J = 8.8$); 7.12−7.19 (m, 6H ArH); 7.27−7.42 (m, 6H, ArH). Anal. Calcd for $C_{29}H_{21}N_3O$: C, 81.5; H, 5.0; N, 9.8. Found: C, 80.07; H, 5.19; N, 9.44.

5-Diphenylamino-2-nitrosophenol Hydrochloride (10). A 4.43 g (18 mmol) portion of **4** was dissolved in a mixture of 10 mL of acetonitrile, 10 mL of concentrated hydrochloric acid, and 6 mL of water, cooled to −5 °C with ice bath. A solution of 1.50 g (22 mmol) of sodium nitrite in 10 mL of 1:1 water/brine was added slowly below the surface of the solution, followed by 5 mL more of brine. The reaction was stirred in the ice bath for 1 h and then water was added to precipitate the product which was filtered and used directly in the next step. ^{1}H NMR ($CDCl_3$, 250 MHz) δ [ppm]: 1.70 (b, 1H, OH); 5.84 (d, $J_{4,6} = 2.5$ Hz, 1H, H^6); 6.45 (dd, $J_{3,4} = 9.8$ and $J_{4,6} = 2.5$ Hz, 1H, H^4); 7.18−7.47 (m, 11H, H^3 + ArH).

9-Diphenylamino-5*H*-benzo[*a*]phenoxazin-5-one (Ph9S). 1-Naphthol **(11)** (3 g (21 mmol)) was mixed with **10** from above and dissolved in 150 mL of dimethylformamide and taken to reflux for 3 h. After cooling to room temperature, the reaction mixture was poured into water and 5% ammonium hydroxide solution was added to neutralize the solution. The product was filtered, washed with water, dried under vacuum to 5.77 g (78% crude yield), and purified by flash chromatography on silica gel using methylene chloride as the eluent, followed by recrystallization from chloroform yielding 1.46 g of purple crystals (20% yield). ^{1}H NMR ($CDCl_3$, 250 MHz) δ [ppm]: 6.32

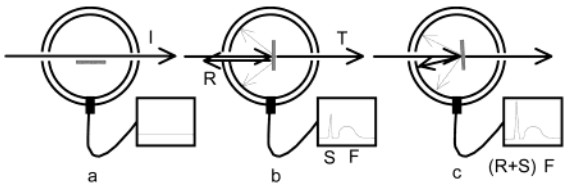

Figure 2. Absolute PLQE measurement.

(s, 1H, H^6); 6.78 (d, $J_{8,10} = 2.5$ Hz, 1H, H^8); 6.92 (dd, $J_{8,10} =$ 8.8 Hz and $J_{10,11} = 2.6$ Hz, 1H, H^{10}); 7.14−7.40 (m, 10H, ArH); 7.58 (d, $J_{10,11} = 8.8$ Hz, 1H, H^{11}); 7.6−7.8 (m, 2H, $H^2 + H^3$); 8.27 (d, $J_{1,2} = 7.8$ Hz, 1H, H^1); 8.65 (d, $J_{3,4} = 6.9$ Hz, 1H, H^4). Anal. Calcd for $C_{28}H_{18}N_2O_2$: C, 81.1; H, 4.4; N, 6.8. Found: C, 81.23; H, 4.60; N, 6.69.

Optical Property Characterization. Photoluminescence (PL) spectra of the dyes in polymer films were obtained by dissolving the dyes in poly(methyl methacrylate) (PMMA) solutions (20 wt % of 20 K polymer dissolved in 1:1 1-methyl-2-pyrrolidinone/1,2-dimethoxyethane), spin-coating onto quartz wafers, and drying on a hotplate at 110 °C under nitrogen atmosphere for 30 min. The absorption spectra were obtained on a Perkin-Elmar Lambda 9 UV/VIS/NIR spectrometer and PL spectra were from a Jobin Yvon Horiba Fluorolog-3 spectrofluorometer. Excitation was at the wavelength of the absorption maxima.

PL Quantum Efficiency Measurements. The PL quantum efficiency of the dye-doped polymer films was measured using an integrating sphere as illustrated in Figure 2. Light from an argon ion laser passes through the sphere along its major diameter (Figure 2a) to a photodetector which, without the sample in place, measures the incident photon flux, I. The sample, on a transparent substrate, is then rotated on its holder such that it is (virtually) normal to the incident beam (Figure 2b). The first detector then is used to measure the transmitted flux, T, and a second photodetector at the entrance aperture is used to measure the reflected flux, R. At the same time an optical fiber couples the light collected by the sphere into a spectrograph, which had been previously calibrated using a quartz-tungsten−halogen bulb of known spectral intensity. The spectrograph is used to determine the scattered flux at the wavelength of the incident laser beam, S, as well as the integrated flux of the fluorescent emission, F. The collection efficiency of the integrating sphere can be cross-checked against the photodetectors by rotating the sample slightly off-normal such that the reflected beam hits the inside surface of the sphere and is collected (Figure 2c). In this geometry, the spectrometer measures the sum ($R + S$) at the laser wavelength.

These measurements permit the determination of the absorbed photon flux, $A = I - (T + R + S)$, and therefore of the PL efficiency, $\Phi_{PL} = F/A$.

Stability. The thermal stabilities of these dyes were evaluated by differential scanning calorimetry to determine T_m and thermogravimetric analysis at a heating rate of 10 °C/min under nitrogen to determine the onset of thermal decomposition, T_d. Relative photooxidative stabilities were determined on the films prepared for absorption and PL spectra. Over a period of two weeks, the films were exposed to ambient room conditions, yellow lights, and/or in the absence of air with periodic reevaluation of the absolute PLQE.

OLED Device Preparation. Dye-doped OLED devices were prepared by dissolving the dyes at 2 mol % concentration into solutions (10 mg/mL in xylenes) of the cross-linkable polymer, styrene-terminated poly(9,9-di-*n*-hexylfluorene) (x-DHF),[38] used for the emitter layer of a two-layer OLED structure. After spin-coating, the polymer was dried at 80 °C to prevent sublimation of the dye from the film. In all cases, the ITO anode was overcoated with PEDOT-PSS (Baytron-P, obtained from Bayer Corp.), the hole transport layer was cross-linked poly(*n*-hexyltriphenylamine) (x-HTPA),[39] and the 250 Å calcium cathode was topped with 300 Å aluminum. OLED fabrication details have been described previously.[39]

EL Characterization. All devices were examined either in the inert atmosphere of a glovebox, or for spectroscopy and microscopy, in sealed canisters through a quartz window. Current−luminance−voltage and efficiency measurements were made using a Keithley model 238 source-measure unit and an Optical Laboratories model 730C intergrating sphere radiometer, as described previously. EL spectra from the entire device were obtained with a Jarrell-Ash 1/4m Czerny-Turner spectrograph, using an EG&G model 1461 photodiode array detector. Fluorescence microscopy was performed using a Nikon Eclipse E400 microscope fitted with an epifluorescence exciter and mercury lamp source. Samples were irradiated with 400 nm radiation, and fluorescence was observed and images were captured using a Nikon digital camera. EL and small spot microscopy were obtained with a home-built microscope system, containing a beam splitter and a pinhole coupler to an optical fiber. By focusing the 10× image of the sample on, for example, a 200 μm pinhole, a 20 μm spot can be evaluated. The optical fiber feeds an Acton Research SpectraPro-150 Czerny-Turner spectrometer, equipped with a SpectrumM 1024 × 128 CCD array detector.

OLED Color Patterning. To demonstrate the feasibility of color patterning by these dopant dyes into a blue-emitting host polymer, we have explored the use of dye transfer via a soft lithographic stamping technique, dry contact dye diffusion.[40] The dyes studied have a limited solubility in cured poly(dimethylsiloxane) (PDMS) resin. Fortunately, only a very small amount of dye needs to be transferred to the polymer surface. The dyes can be loaded into PDMS via two methods. The first loading method examined was incorporation of the dye by solvent-assisted dissolution of the dye with the uncured PMDS resin, followed by solvent removal and thermal curing. Accordingly, a 10-mL glass vial was charged with 2.0 mg of C7S and 1.0 g of CH_2Cl_2, and the contents were stirred. To this solution was added 8.7 g of Sylgard 184 resin. The resin and dye solution were allowed to mix for 1 h. The solvent was removed in vacuo, and Sylgard curing agent activator was added (10 wt %). The dye-doped PDMS mixture was stirred vigorously for three minutes and then degassed. The mixture was carefully poured onto the silicon master and cured in an oven at 80 °C for 20 h. The stamp was easily peeled off of the master and stored on a clean glass slide. Upon observation, the dye was well dispersed through the PDMS stamp and showed signs of slight crystallization within the stamp. Alternatively, blank PDMS was cast from the patterned master (resin heated at 60 °C for 12 h). After release from the master the blank patterned stamp was immersed in a solution of C7S (10 mg/mL in toluene) for 30 min. The dye infused into the PDMS matrix and the resulting stamp was heated for 1 h at 60 °C to remove residual solvent. EL devices were prepared using x-HTPA as the hole-transport layer and xDHF as the electron-transport /emitter layer. Printing was done after casting and drying the polyfluorene. Contact of the stamp onto the substrate was made for several minutes at 60 °C.

Results and Discussion

Synthesis. The synthesis scheme for the coumarin dye series is shown in Scheme 1. *m*-Anisidine was coupled with iodobenzene using a phase transfer variant of the Ullmann[41] procedure to prepare ether **3** which was cleaved using freshly prepared aluminum iodide to phenol **4** followed by condensation[42] with diethyl

(38) Klaerner, G.; Lee, J.-I.; Lee, V. Y.; Chan, E.; Nelson, A.; Markiewicz, D.; Chen, J. P.; Siemens, R.; Scott, J. C.; Miller, R. D. *Chem. Mater.* **1999**, *11*, 1800.

(39) Chen, J. P.; Klaerner, G.; Lee, J.-I.; Markiewicz, D.; Lee, V. Y.; Miller, R. D.; Scott, J. C. *Synth. Metals* **1999**, *107*, 129.

(40) A separate paper detailing 3-color OLED devices made by dry contact dye diffusion is being prepared and will follow publication of this manuscript.

(41) Gauthier, S.; Fréchet, J. M. J. *Synthesis* **1987**, 383.

(42) Bissell, E. R. *Synthesis* **1982**, 846.

Scheme 1. Synthesis of Diarylamine Substituted Coumarin Dyes

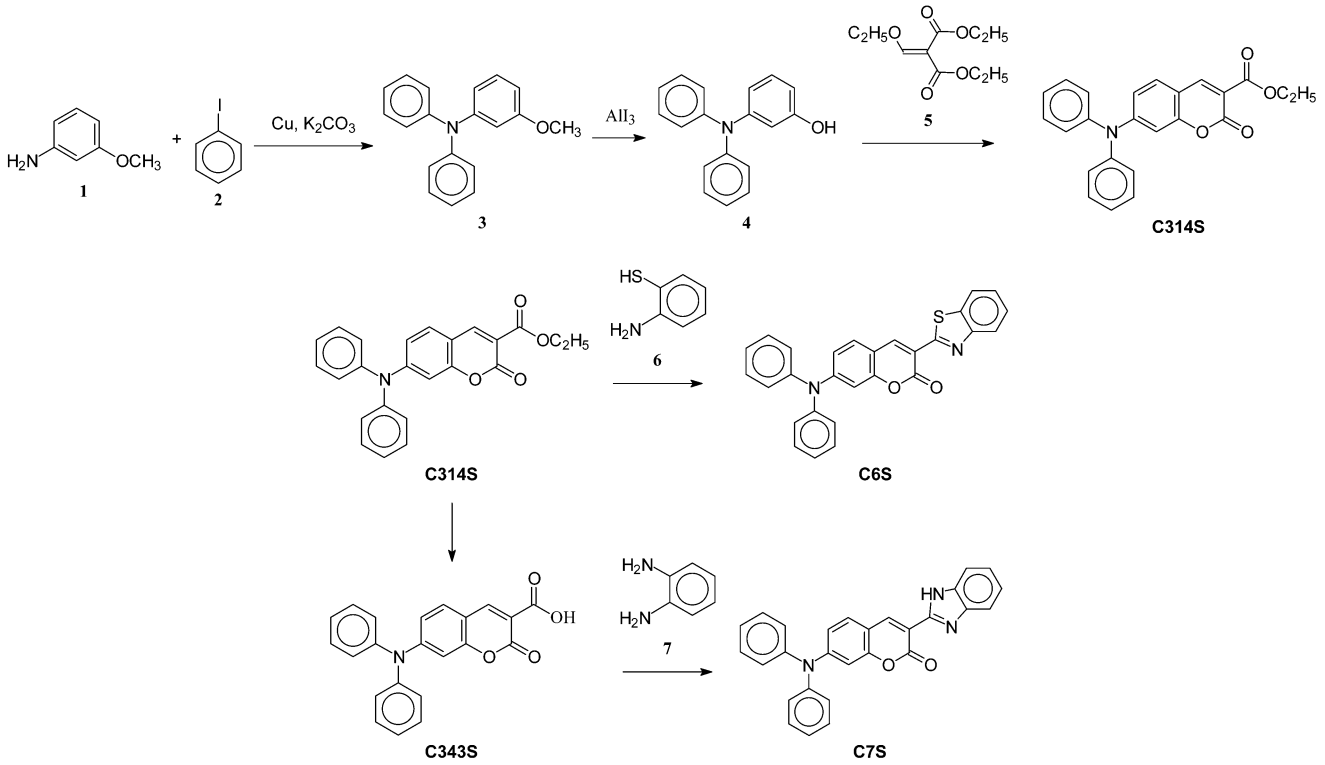

Scheme 2. Synthesis of Diarylamine Substituted DCM (DCMS) and Its Dimer, DADP

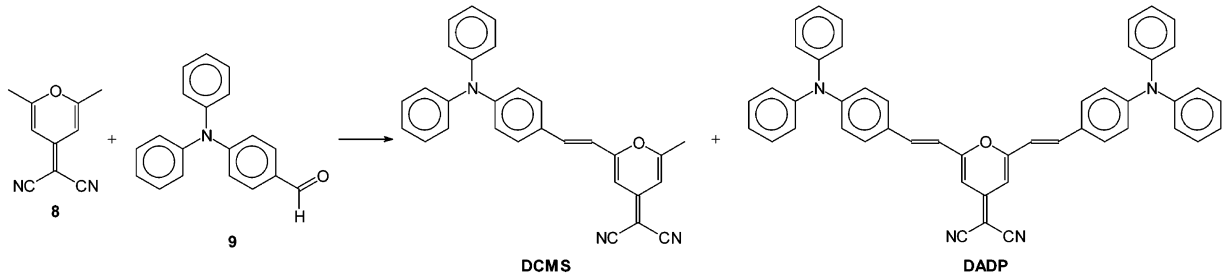

Scheme 3. Synthesis of Diarylamine Substituted Phenoxazone 9 (Ph9S)

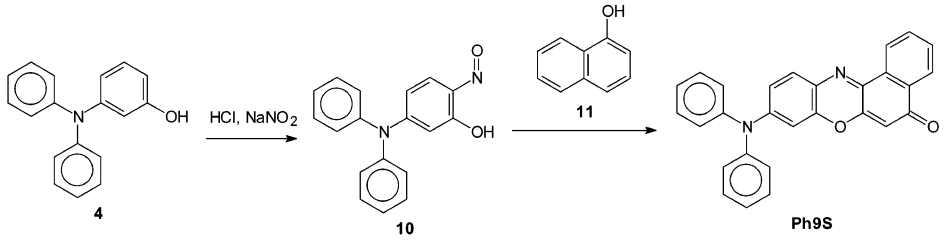

ethoxymethylenemalonate (**5**) to provide C314S in 45% yield. C6S was prepared by the thermal condensation[43] of 2-aminothiophenol (**6**) with C314S in 10% yield from *m*-anisidine. C314S was hydrolyzed to C343S followed by dehydration and condensation[44] with *o*-phenylenediamine (**7**) to yield C7S in 3% yield from *m*-anisidine. DCMS was prepared as described for other DCM analogues[45] in 5% yield and is shown in Scheme 2. The synthesis of the Ph9S is shown in Scheme 3. Nitrosation of phenol **4** followed by condensation[46] with 1-naphthol **11** yielded Ph9S in 20% yield from *m*-anisidine.

PL Properties for External Color Conversion. The choice of materials for external color converter layers requires balancing an array of interrelated elements including the choice of the dye(s) itself, the polymer matrix, the casting solvent (film quality), the concentration of the dye relative to the polymer and to the casting solvent, the processing conditions, temperature limits, and the effects of each of these on the optical properties (the absorption and emission spectra) of the films. For efficient external conversion, the fluorescent dye should have an absorption spectrum that overlaps with the (blue) EL spectrum of the emitter as well as efficient red or green PL emission. PL spectra

(43) Haeusermann, H.; Voltz, J. German Patent 1,098,125, 1959; *Chem. Abstr.* **1962**, *56*, 10158.
(44) Hendrickson, J. B.; Hussoin, M. S. *J. Org. Chem.* **1987**, *52*, 4139.
(45) Bourson, J.; Valeur, B. *J. Phys. Chem.* **1989**, *93*, 3871.
(46) Simmonds, A.; Miller, J. N.; Moody, C. J.; Swann, E.; Briggs, M. S. J.; Bruce, I. E. WO 97/29154, 1997.

Table 1. Optical Properties of 5 wt % Dyes in Polymer Films

dye	λ_{max} ABS (nm)	λ_{max} PL (nm)	PLQE
C314S	420	525	61%
C343S	431	560	
C6	445	530	31%
C545T	476	532	
C6S	447	544	78%
C7	436	505	
C7S	435	522	75%
DCM	466	599	
DCJTB	499	565	
DCMS	457	585	
DADP	474	585	
Ph9	516	612	
Ph9S	527	600	

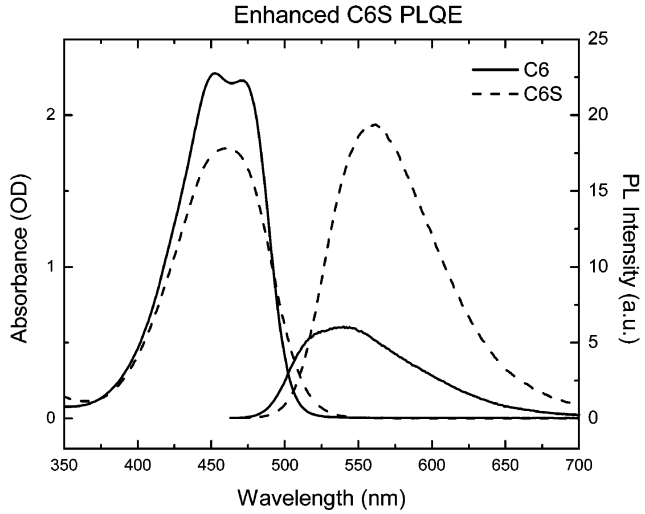

Figure 3. Absorption and PL spectra of C6 and C6S in polymer films.

of coumarin-S dyes dissolved in polymer films showed significant luminescent intensity increases over their commercial analogues at the same concentration. The coumarin-S dyes had PLQE values of 60−80%, easily twice that of their commercial analogues and similar to that of the coumarin-T dyes (Table 1 and Figure 3).

It can be a challenge to optimize the absorption without quenching the emission due to concentration effects. Although laser dyes have very high (>90%) fluorescence efficiencies when dilute, at higher concentrations (corresponding to a mean dye molecule separation of <5−10 nm) the internal fluorescence efficiencies may drop due to the resonant energy transfer process known as Förster transfer.[47] The effect of concentration quenching on the photoluminescence of DCM can be seen in Figure 4. The high concentrations of dye needed for absorption lead to PL quenching and color-shifts. Concentration quenching effects have been shown to be reduced by steric spacer structural modifications such as the methyl groups in DCJT.[48] The S-type dyes with their bulky diphenylamino groups show similar behavior. The PL intensity of films of DCMS begins to decline above 5 wt % concentration compared to 0.5% for DCM. Similarly, the PL intensity of C6S films reaches a maximum at about 5 wt % concentration compared to 2.5% for C6.

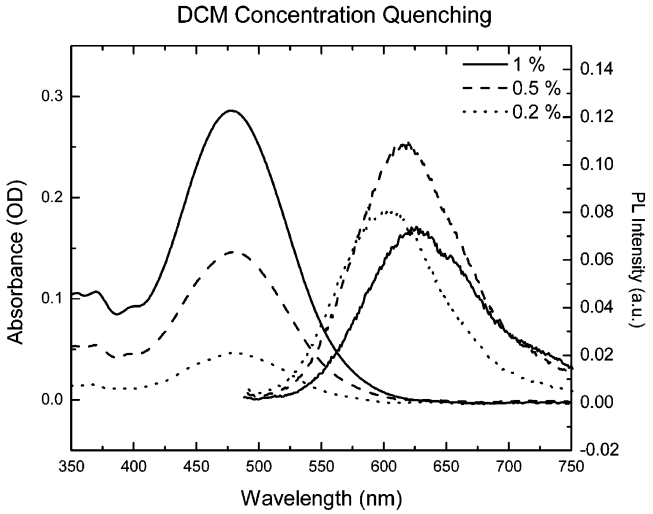

Figure 4. Absorption and PL spectra of DCM vs concentration. Although the dye follows Beer's Law in absorbance, the PL is diminished as the concentration increases above 0.5% in the polymer film. The PL wavelength maxima also red-shifts as the concentration increases.

Concentration quenching can be further reduced by the addition of small amounts of a second fluorescent dye in the converter film (host-doping). The blue emission is thus absorbed by the more concentrated dye and transfers via the Förster process to a second dye which controls the PL properties of the film. The concentration of the dopant dye can be optimized to minimize the concentration quenching effect.[49,50] This cascade process has the additional advantage that one dye can be selected for maximal overlap with the blue emission while the emission of the second dye can be selected for optimal red or green color coordinates. Using this host−dopant approach, conversion of blue light to red and green by external color converters was achieved as shown in Figure 5.

The PLQE values of the coumarin-S dyes showed improved photooxidative stability as shown in Figure 6. Films of C6S in PMMA lost only 9% of their PLQE, whereas C6 films lost 35% of their original PLQE value when subjected to ambient (air atmosphere under fluorescent lights) conditions over a two week period.

The replacement of dialkylamino groups with diarylamine moieties in dyes has been shown to result in increased thermal stability.[51] The thermal properties of these dyes as evaluated by DSC and TGA to determine T_m and T_d are compared in Table 3. The S-class dopants have higher decomposition onset temperatures than their commercial dialkylamino analogues or the tetramethyl julolidyl (T-class) analogues. This stability should reduce thermal decomposition during resistively heated vacuum deposition processes.

External Color Converter Fabrication. External conversion also requires the fabrication of a thin-film conversion layer with red and green elements patterned to match the size of the pixel structure. To avoid interpixel cross-talk or excitation into near neighboring converter pixels, the converter layer must be thin relative to the pixel dimensions and positioned as close

(47) Yardley, J. T. *Introduction to Molecular Energy Transfer*; Academic: New York, 1980; p 234.
(48) Chen, C. H.; Tang, C. W. *Proc. 2nd Int. Symp. Chem. Function. Dyes* **1992**, 536.
(49) Guha, S.; Haight, R. A.; Bojarczuk, N. A.; Kisker, D. W. *J. Appl. Phys.* **1997**, *82*, 4126.
(50) Jones, G.; Morais, J. *Proc. SPIE* **1996**, *2698*, 65.
(51) Moylan, C. R.; Twieg, R. J.; Lee, V. Y.; Swanson, S. A.; Betterton, K. M.; Miller, R. D. *J. Am. Chem. Soc.* **1993**, *115*, 12599.

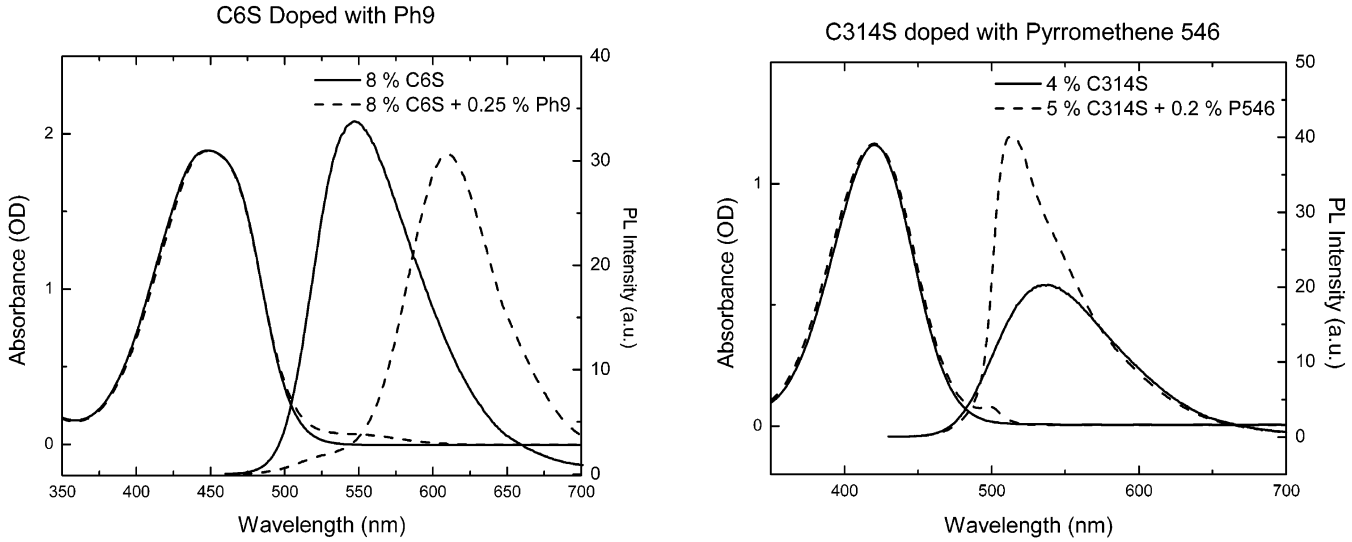

Figure 5. Absorption and PL spectra of red and green external color conversion films. The coumarin-S dyes act as hosts absorbing the blue emission. The PL is tuned by the dopant dyes, Ph9 for red and P546 for green.

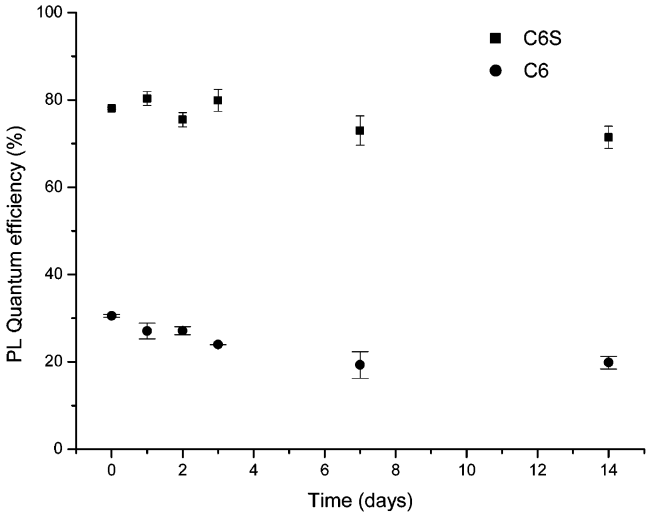

Figure 6. Stability of PL quantum efficiency for 5 wt % C6 (●) and C6S (■) in PMMA films.

Table 2. Electroluminescence (EL) Properties of 2 Mol % Dye Doped OLEDs

dye	λ_{max} EL (nm)	OLED QE (cd/A) (% photons/ charge carrier)	OLED power efficiency (lm/W)
undoped	425	0.22 (0.36)	0.090
C6	482	0.532 (0.242)	0.239
C545T	496	0.278 (0.097)	0.131
C6S	507	0.598 (0.194)	0.272
C7	506	0.182 (0.078)	0.091
C7S	499	0.711 (0.253)	0.299
DCM	561	0.142 (0.059)	0.068
DCJTB	563	0.342 (0.116)	0.162
DCMS	567	0.283 (0.098)	0.13
DADP	567	0.385 (0.143)	0.237
Ph9	565	0.297 (0.149)	0.135
Ph9S	582	0.179 (0.077)	0.072

to the emitting layer as possible. There is also the potential problem of "color bleeding" when light is waveguided in the converter substrate itself and unintentionally excites neighboring pixels which further complicates this strategy. Standard lithographic patterning techniques were used to fabricate an external converter structure into pixel-sized features on a separate substrate as shown in Figure 1a. An alternate strategy would be to position the converter as the bottommost structure in the device stack (i.e., covered with a transparent electrode followed by the rest of the OLED layers). Alternatively, the converter structure could be fabricated directly on the OLED device but much care is required not to damage the underlying OLED and electrode layers which are sensitive to aqueous solutions and many solvents.

Table 3. Thermal Properties of Fluorescent Dyes

dopant	T_m (°C)	T_d (°C)
C314T	132	261
C314S	37.5	264
C343S	288	307
C6	212	320
C545T	234	333
C6S	240	344
C7	242	305
C7S	247	357
DCM	227	307
DCMS	230	344
DCJTB	303	325
Ph9	212	271
Ph9S	229	318

EL Properties and OLED Device Characteristics. For internal conversion, the emission from the dopant dye must be of lower energy than that of the active layer so that down-conversion will occur. Similar to external conversion, the emission of the dopant should be at the desired wavelength (red or green). In this case, after the excitation of the host material, Förster transfer allows the excitation to be transported through the host until it reaches a dopant molecule which relaxes radiatively by emission of a photon resulting in color down-conversion. Likewise, concentration quenching effects can occur in the internal dye-doping scheme, and dopant concentrations can be adjusted to minimize quenching and optimize the desired emission.

The EL spectra of the dye-doped OLEDs are shown in Figure 7. The polyfluorene host, x-DHF, was chosen for its highly efficient emission and good blue CIE coordinates before doping. Exciton transfer to or creation on the coumarin dyes was fairly efficient with little blue emission from the x-DHF observed at 426 nm (Figure 7a) and was most efficient to the S- and T-class dyes. Transfer to DCM (Figure 7b) was inefficient but

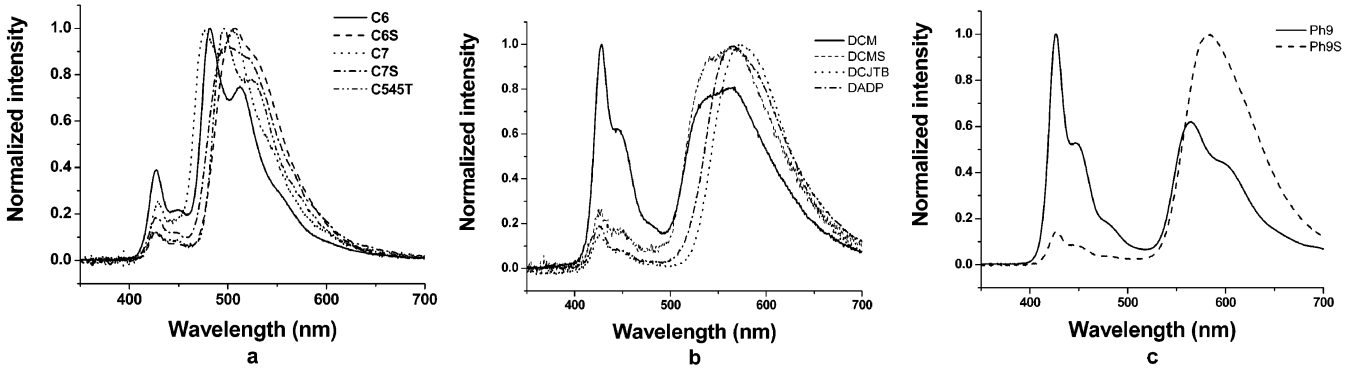

Figure 7. EL spectra of OLEDs doped with 2 mol % (a) coumarin, (b) (dicyanomethylene)pyran, and (c) benzophenoxazone dyes.

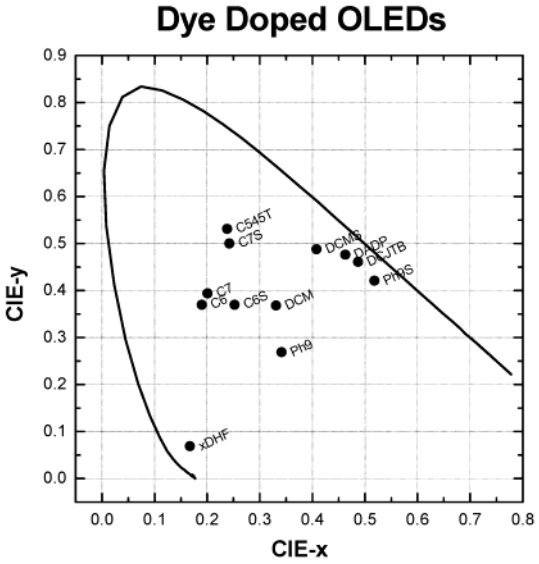

Figure 8. CIE coordinates of dye-doped OLEDs.

significantly improved in the S- and T-derivatives. Similarly, transfer to Ph9 was poor but significantly improved in Ph9S (Figure 7c).

The Commission Internationale d'Eclairage (CIE) coordinates of the emission from the dye doped OLEDs are shown in Figure 8. The inefficient transfer from x-DHF to DCM and Ph9 is again evident in the whiteness of the color coordinate positions due to the blue component in the emission.

The external quantum and power efficiencies of the dye-doped OLEDs are summarized in Table 2, and in most cases the S- and T-derivatives are more efficient. Only the Ph9S exhibits degraded efficiency which may be more indicative of the large energy difference between the OLED material and the red dye.

Color OLED Patterning. Dopant dyes may be patterned into polymer emitters via soft-lithographic stamping,[52] ink-jet from solution,[53,54] masked dye diffusion,[55,56] or maskless dye diffusion.[57] Internal conversion or dye doping has the potential for much higher efficiency due to the close coupling of the excitation, transfer to the dopant and radiative emission, and the lack of emission/absorption steps required in external conversion.

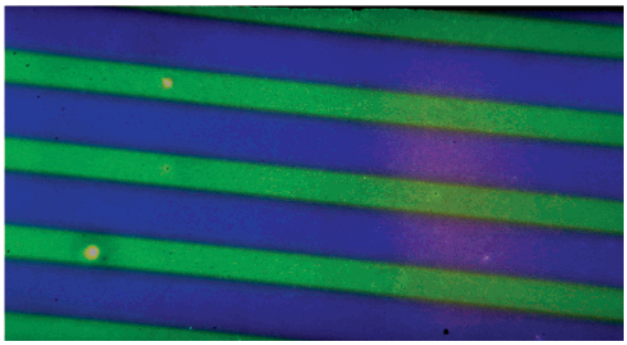

Figure 9. EL image of OLED with doped C7S Pattern.

The transfer of the green dopant dye, C7S, into the blue-emitting host polymer, x-DHF, in a striped pattern by soft lithographic stamping is demonstrated by the EL image shown in Figure 9. The stamp was prepared by the second described technique (dye was infused into a preformed blank PDMS stamp via immersion in the dye solution). The stamp patterns and the green stripes are 80 μm wide at 240 μm repeat distance, resulting in an OLED with both green and blue patterned regions. These results show that dry contact dye diffusion may provide an attractive alternative procedure for the creation of 3-color OLED devices. This technique has been further developed and will be the subject of a forthcoming manuscript.[40]

In summary, a series of diphenylamine substituted coumarin, (dicyanomethylene)pyran, and benzophenoxazone dyes have been synthesized, and their optical and electroluminescent properties and thermal and photooxidative stabilities have been investigated and compared to those of their commercial analogues. The incorporation of bulky phenyl groups delays the onset of concentration quenching, and their improved photoluminescent efficiency and photooxidative stability make them excellent candidates for external color-conversion materials. Improved electroluminescence and power efficiencies and enhanced thermal stabilities suggest their use as dopants in OLEDs. In particular C7S is an excellent choice as a green dopant for use in OLED displays.

Acknowledgment. This work was partially supported by a grant from the National Science Foundation (CHE-9625628).

CM021056Q

(52) Chen, J. P.; Salem, J. R.; Scott, J. C. U.S. Patent 6,214,151, 2001.
(53) Bharathan, J.; Yang, Y. *Appl. Phys. Lett.* **1998**, *72*, 2660.
(54) Hebner, T. R.; Sturm, J. C. *Appl. Phys. Lett.* **1998**, *73*, 1775.
(55) Bao, Z.; Campbell, S. *Thin Solid Films* **1999**, *352*, 239.
(56) Pschenitzka, F.; Sturm, J. C. *Appl. Phys. Lett.* **1999**, *74*, 1913.
(57) Tada, K.; Onoda, M. *Jpn. J. Appl. Phys.* **1999**, *38*, L1143.